Third-Order First-Harmonic Wave Excitation Forces on Spherical Geometries

Bryan Tan[1], **Jana Orszaghova**[1,2], **Hugh Wolgamot**[1], **Adi Kurniawan**[1], **J. H. Todalshaug**[3]

1. Oceans Graduate School, University of Western Australia, Crawley, WA, Australia
2. Blue Economy Cooperative Research Centre, Launceston, TAS, Australia
3. CorPower Ocean, Stockholm, Sweden

Email: bryan.tan@research.uwa.edu.au

1 Introduction

Higher-order wave-structure interactions are generally investigated to improve the estimation of super- and sub-harmonic forcing relevant to high-frequency structural responses in fixed offshore structures and low-frequency motion responses of soft-moored floating structures. However, far fewer studies have been conducted on higher-order interactions within the wave frequency range which is of primary interest to wave energy devices tuned to resonate within this range.

We experimentally investigate nonlinear effects in first-harmonic wave excitation forces on a fixed sphere of radius $a = 0.125$ m, representative of an archetypal heaving point absorber at reduced scale. The experiments were conducted in a large wave flume at the Coastal and Offshore Research Laboratory at the University of Western Australia. To excite the response, we used incident focused wave groups derived from underlying JONSWAP spectra representative of a range of operational conditions. To probe nonlinearities, we utilised wave groups with progressively higher focus amplitudes. We considered three peak periods and a range of model drafts, but for brevity only show a subset of the results here. We find that third-order first-harmonic forces are readily apparent and for heave in longer waves can be as large as 8% of the peak force in energetic operational conditions. This is primarily induced by the cubic relationship between the spherical cap's volume and draft.

2 Harmonic Structure and Separation

The total wave excitation force (and wave elevation) up to third-order can be decomposed into individual harmonic terms according to a Stokes' harmonic structure

$$F = F^{(11)} + F^{(20)} + F^{(22)} + F^{(31)} + F^{(33)} + \mathcal{O}(A^4), \tag{1}$$

where $F^{(mn)}$ is the m^{th}-order n^{th}-harmonic term, i.e., $F^{(mn)}$ scales with the wave amplitude A raised to the m^{th} power and in the frequency domain is located around $n \times f_p$, with f_p denoting the incident wave peak frequency. For broad-banded incident waves, these terms often overlap in the frequency domain. For this reason, we carried out phase-manipulated tests (nominally crest- and trough-focused incident wave groups) and applied two-phase harmonic separation [1] with frequency-filtering to isolate individual harmonic terms. However, this technique cannot separate the first-order first-harmonic (linear) term $F^{(11)}$ from the third-order first-harmonic term $F^{(31)}$ as they have identical phase dependence and span the same frequency range. This inseparability of the first-harmonics is key to interpreting the nonlinear features in the results.

3 First-Harmonic Time Series

The experimentally measured first-harmonic forces $F^{(11)} + F^{(31)}$ and waves $\eta^{(11)} + \eta^{(31)}$ are extracted by band-pass filtering the odd harmonics between $0.7f_p$ and $2.5f_p$. Figure 1 shows the first-harmonic force time series induced by five incident wave groups of varying focus amplitudes, normalised by the envelope peak of the measured first-harmonic incident wave $\hat{A}$. The lighter lines correspond to higher amplitudes. As expected, the general collapse of the lines from this amplitude normalisation shows that the content is primarily linear, but more interestingly, the amplitude ordering of the residuals suggests that nonlinear contributions are also observable. Note that this ordering does not appear noticeably in the wave elevation time series, which we

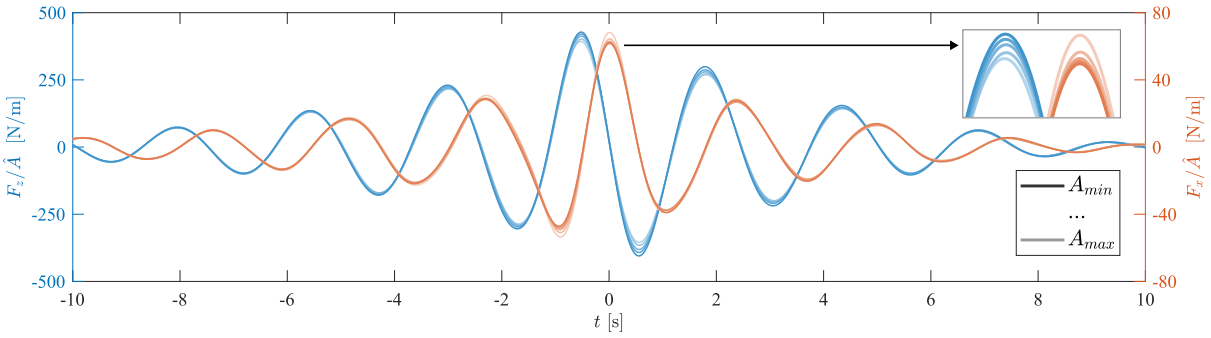

Figure 1: Experimentally extracted normalised first-harmonic force time series for a half-submerged sphere. Nominal linear focus amplitudes of $A = \{0.010, 0.025, 0.040, 0.060, 0.080\}$ m and peak frequency of $f_p = 0.40$ Hz, in a water depth of $h = 1.1$ m.

do not show here. For the heave force F_z plotted in blue, the normalised first-harmonic force reduces with increasing incident wave amplitude. The surge force F_x plotted in orange shows the opposite behaviour. These separations appear most prominently in the centre of the wave group, indicative of nonlinear contributions which are more localised in time than the linear term, consistent with the nonlinear terms' broader frequency bandwidths as a result of 'spectral smearing' [1] due to the increasing number of frequency component interactions. These effects are therefore even more pronounced in the frequency domain which we show using transfer functions.

4 First-Harmonic Transfer Functions

The wave-to-force transfer function is calculated as the ratio between the complex amplitudes of the force and the undisturbed wave elevation. We define the first-harmonic transfer function $\mathcal{F}^{(1)}$ as below, which in addition to the linear terms also contains higher-order first-harmonic terms from the two-phase harmonic separation method:

$$\mathcal{F}^{(1)} = \frac{\tilde{F}^{(11)} + \tilde{F}^{(31)} + \mathcal{O}(A^5)}{\tilde{\eta}^{(11)} + \tilde{\eta}^{(31)} + \mathcal{O}(A^5)} \approx \frac{\tilde{F}^{(11)}}{\tilde{\eta}^{(11)}} + \mathcal{O}(A^2), \tag{2}$$

where $\eta^{(mn)}$ is the wave elevation term with identical notation to the forces, and the $\tilde{}$ accents denote the complex amplitude of the quantity (note that we cannot isolate $\eta^{(31)}$). The experimental first-harmonic transfer function amplitudes for $f_p = 0.40$ Hz and 0.80 Hz ($k_p a \simeq 0.1, 0.3$, respectively) are plotted in Fig. 2, along with the theoretical purely linear transfer function amplitudes calculated from linear potential flow theory [2]. The progressively increasing deviation of the experimental first-harmonic transfer functions $\mathcal{F}^{(1)}$ from the theoretical linear curve can be clearly seen for heave in long waves and surge in short waves. Furthermore, these deviations appear to be minimised at the peak frequency and increase towards the tails of the spectrum. Such features are indicative of a higher-order term within the first-harmonic frequency range: while the linear term is dominant, its bandwidth is limited compared to higher-order terms which contribute increasingly larger portions of the first-harmonic force away from the peak frequency. The effects of the nonlinear contributions are therefore much more noticeable at the tails of the spectra whereas the linear content dominates around the peak frequency. To elucidate the origin of this nonlinearity, we investigate the amplitude dependence of the transfer function deviations (assuming the smallest amplitude case to be the nominally linear reference and evaluating the differences in the frequency domain averaged over the high-frequency tail $[1.6, 2.1]f_p$). Fig. 3 shows the predominantly quadratic behaviour of the transfer function separations corresponding to third-order nonlinearity, as indicated by Eq. 2. We note that Morison-type viscous drag terms can also occur in the first-harmonic range but would exhibit quadratic amplitude dependence (i.e. linear trends in Fig. 3). The observed nonlinearity therefore appears to be a cubic effect.

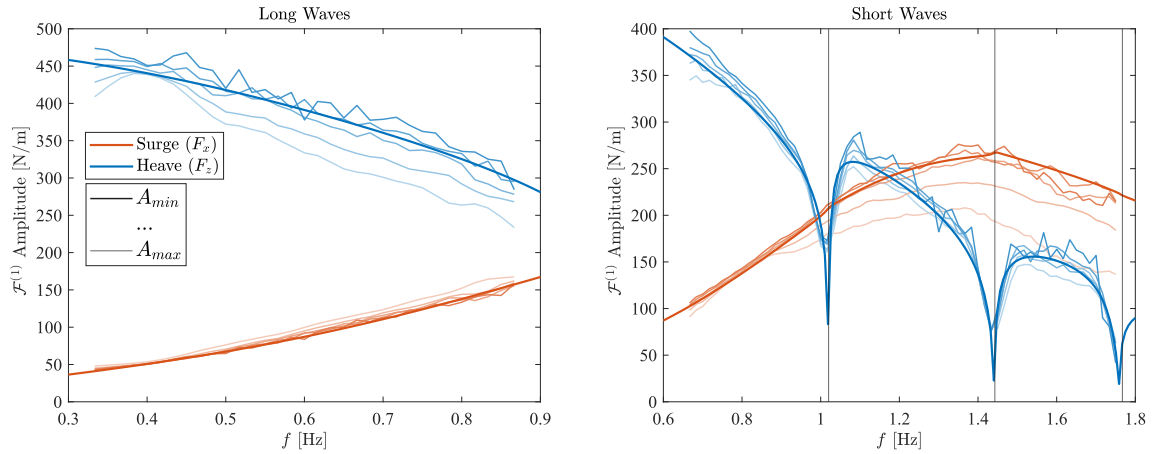

Figure 2: Experimentally extracted first-harmonic wave-to-force transfer function amplitudes (thin lines) and theoretical linear transfer function amplitudes from linear potential flow theory (bold lines). Peak frequencies $f_p = 0.40$ Hz (left) and 0.80 Hz (right). The black vertical lines denote the flume cross-modes.

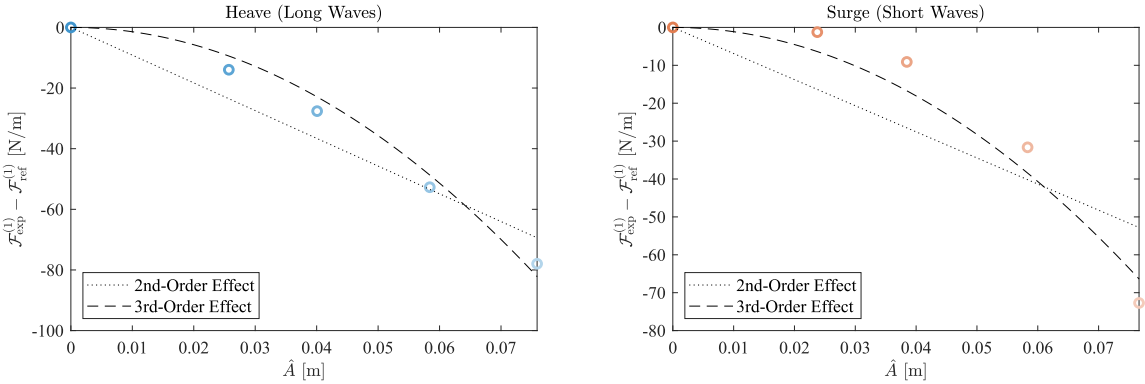

Figure 3: Separation of the transfer functions from the reference (smallest amplitude transfer function) as a function of the incident wave amplitudes, averaged from $1.6f_p$ to $2.1f_p$, for heave and surge in long and short waves respectively. Polynomial fits demonstrate the order of the separation.

5 Understanding the Third-Order First-Harmonics Using Simple Models

Wave energy developers require simple hydrodynamic models for real-time control. We therefore investigate, using simple corrections, which terms contribute to these cubic effects. For long waves, almost all of the nonlinear behaviour for the heave force is explained by including the instantaneous buoyancy force $\rho g V(t)$ below the undisturbed first-harmonic free surface (assumed to be constant across the body). As previously mentioned, this is because of the cubic relationship between the spherical cap's volume and draft. Interestingly, this correction is not appropriate in the short waves. Including simple small-body nonlinear Froude-Krylov (FK) terms, incorporating an instantaneous submerged volume and evaluating kinematics at the submerged centroid, is sufficient to capture much of the effect for surge forces in short waves. Here the measured first-harmonic undisturbed wave elevation at the centre of the sphere was used to calculate the linear kinematics and then the theoretical second-order bound waves and kinematics from second-order wave-wave interaction theory [3] were added. Using both corrections, the same two-phase harmonic separation method used above was applied to the numerical results, such that the simulated first-harmonic transfer functions are extracted and compared to the experimental results in Fig. 4. It may be seen that the FK terms only partially reproduce the observed nonlinearities for surge in short waves. Computations suggest that including simple small-body approximations for nonlinear diffraction can further improve the agreement. These and corresponding results for different drafts will be presented at the workshop.

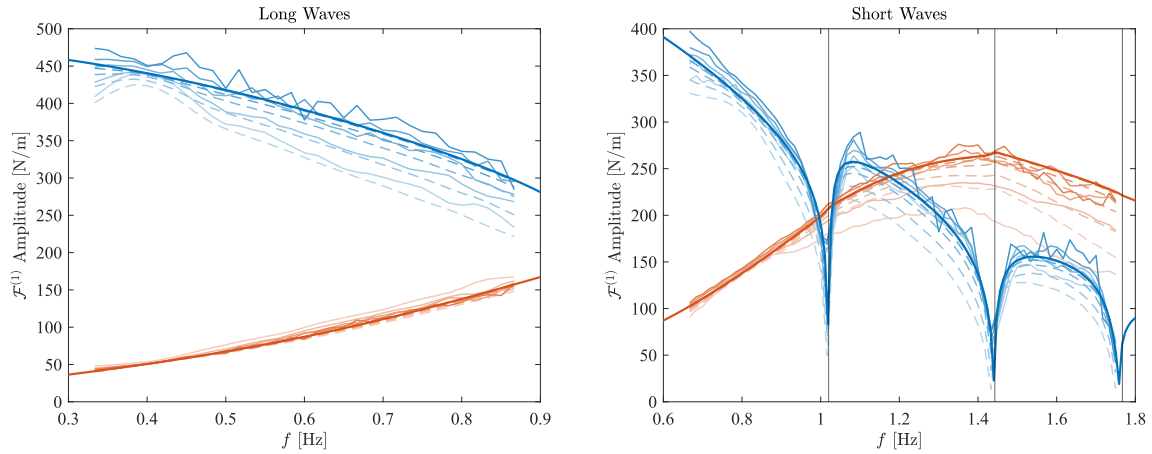

Figure 4: Experimental (solid thin lines) and numerical (dashed thin lines) first-harmonic transfer function amplitudes incorporating instantaneous buoyancy and nonlinear FK terms. Peak frequencies of $f_p = 0.40$ Hz (left) and 0.80 Hz (right). The black vertical lines denote the flume cross-modes.

6 Conclusions

A careful experimental investigation of excitation forces on fixed spherical bodies was conducted in a wave flume to improve understanding of nonlinear wave-body interactions for wave energy applications. Two-phase harmonic separation was used to process the data and isolate the first-harmonic where noticeable nonlinear effects were observed in the forces. We note that the characteristic spectral broadening of the nonlinear correction is apparent in these tests but would not (by definition) be visible in regular waves, and would likely be corrupted by reflections in irregular waves or by even harmonics if phase separation were not used. Using scaling arguments, the nonlinear features are shown to be due to third-order difference-frequency effects rather than drag. These terms can therefore be approximately modelled relatively efficiently, albeit that there is currently no general third-order diffraction theory available for validation [4]. Such third-order difference frequency effects have occasionally appeared in previous studies [5]. However, we expect these third-order first-harmonic terms to be of interest in the context of resonating wave energy converters, especially when similar effects due to large body motions (typically > free surface motions) as well as various wave-motion forcing cross-terms [6] are considered.

7 Acknowledgements

This work is funded by the ARC (LP210100397), a UWA Research Impact Grant, and the Blue Economy Cooperative Research Centre CRC-20180101. BT is supported by the Aus. Gov. RTP Fees Offset and Stipend at UWA. HW is supported by Shell Australia. AK is supported by MERA, jointly funded by UWA and the Western Aus. Gov. Dr Guy McCauley and George Ellwood assisted with the experiments.

References

[1] C. J. Fitzgerald *et al.*, "Phase manipulation and the harmonic components of ringing forces on a surface-piercing column," *P R Soc A*, vol. 470, 2014. DOI: 10.1098/rspa.2013.0847.

[2] WAMIT, *User manual*, Version 7.4, WAMIT, Inc., 2020.

[3] J. Dalzell, "A note on finite depth second-order wave-wave interactions," *Applied Ocean Research*, vol. 21, no. 3, pp. 105–111, 1999. DOI: 10.1016/S0141-1187(99)00008-5.

[4] S. Malenica and B. Molin, "Third-harmonic wave diffraction by a vertical cylinder," *Journal of Fluid Mechanics*, vol. 302, pp. 203–229, 1995.

[5] J. Newman, "Nonlinear scattering of long waves by a vertical cylinder," in *Waves and nonlinear processes in hydrodynamics*, Springer, 1996, pp. 91–102.

[6] H. Wolgamot *et al.*, "Phase-manipulation with multiple controlled inputs to enhance investigation of nonlinear hydrodynamic effects," in *IWWWFB*, Ann Arbor, MI, USA, 2023.